communications earth & environment

Article

https://doi.org/10.1038/s43247-025-02030-9

Scale-dependent responses to environmental fluctuations in tropical tree species' crown temperatures

Check for updates

Shannon L. J. Bayliss[1,2] ✉, Eben N. Broadbent[3], Angélica M. Almeyda Zambrano[4], Susan Cordell[5] & Stephanie Pau[1,2,6]

Tropical forests may be nearing critical temperatures, yet tree species may respond differently. Using high-resolution thermal, hyperspectral, and LiDAR imagery, we mapped 652 crowns of four Hawaiian tree species to study the effects of crown traits and abiotic conditions on species' temperatures at two scales (whole crown vs. sunlit leaves). We show scale-dependent, species-specific relationships with environmental fluctuations. Net radiation was consistently the dominant determinant of crown temperature deviations from air temperature (Tdiff), while vapor pressure deficit, wind speed, and crown traits (e.g., roughness) varied in importance by species and scale. Species explained 17% and 44% of Tdiff variation at the crown and leaf scales, respectively, after controlling for climatic factors. Findings suggest that leaf temperatures overestimate larger-scale temperature differences, while canopy-scale observations underestimate leaf heat stress. Because leaf and crown traits can have opposing effects on Tdiff, disentangling these can advance our understanding of species' thermoregulation under climate change.

Tropical forests are often thought to be generally stable environments because they experience smaller climatic fluctuations compared to higher latitudes[1]. Yet this means that tropical species may be especially sensitive to warming temperatures because they have evolved within a narrow temperature range[1]. Recent work using pantropical satellite data has suggested that tropical tree canopies may already be nearing the critical temperatures at which their photosynthetic machinery is damaged[2], and heatwaves that are increasing in frequency and intensity may push these ecosystems past their critical limits more regularly[3] with implications for ecosystem function[4]. Thermal remote sensing across several sites from different biomes has revealed that tropical canopies are particularly slow to overcome radiative heating through transpiration compared to forests in other biomes, in part because of their leaf and canopy traits[5].

Sunlit leaf temperatures within tree canopies can exceed air temperatures by over 10 °C, and under certain conditions and times of day, these differences can approach 20 °C[6–12]. However, while leaf temperature information is useful, it does not reflect whole-organismal temperatures which are determined by a more complicated set of biotic and abiotic factors[13]. Direct measurements of forest canopy temperatures (T_{can}) through remote sensing can capture heterogeneity across leaves within individual tree crowns and across tree crowns within and among species[14]. While the abiotic drivers of T_{can} are well established[14,15], the same abiotic environment can affect individual species differently because of their distinct leaf and canopy traits, which in turn enable them to uniquely respond to changing environmental conditions[16,17].

Most work on canopy temperature has focused on thermal variation of sunlit crowns within and across sites[2,5,18], rather than within (but see ref. 19) and across species[12,16,18,20]. Yet tree species vary considerably in both leaf and crown architecture traits, which can independently affect how much organismal temperature departs from air temperature[16,21,22]. Furthermore, trait variation within species can rival variation across species with equally large effects on ecosystem functioning. The thermal properties of individual trees and forested ecosystems are influenced by leaf traits such as leaf size, thickness, pigmentation, and stomatal behavior[9,20,23–25]. For example, larger leaves can absorb more heat, and stomatal conductance can control transpirational cooling[9]. Tree crown architectural traits like leaf angle (orientation), crown density, clumping or branching patterns, and surface roughness or rugosity can also impact the distribution of heat and energy absorption in forest canopies[15]. Denser tree crowns often exhibit larger differences from air temperatures due to reduced turbulent heat exchange

[1]Department of Environmental Science, Policy and Management, University of California, Berkeley, Berkeley, CA, 94704, USA. [2]Department of Geography, Florida State University, Tallahassee, FL, 32306, USA. [3]School of Forest, Fisheries & Geomatics Sciences, University of Florida, Gainesville, FL, 32608, USA. [4]Center for Latin American Studies, University of Florida, Gainesville, FL, 32608, USA. [5]Institute of Pacific Islands Forestry, Pacific Southwest Research Station, USDA Forest Service, Hilo, HI, 96720, USA. [6]Department of Geography, University of California, Berkeley, Berkeley, CA, 94704, USA. ✉e-mail: shannonljbay@gmail.com

between sensible and latent heat between the canopy and air[7,16,18], and rougher crowns can enhance turbulent air mixing between layers resulting in higher coupling between tree and air temperatures[15]. Uneven canopies can also absorb more radiation throughout canopy layers because scattered light can be absorbed in lower layers. Crown architecture also affects the distribution and proportion of sunlit and shaded leaves. These crown-level traits are increasingly recognized as capturing important adaptive responses to global change[14,26].

Disentangling the influence of leaf and whole-crown architecture on forest temperature dynamics is critical for understanding the ways that species may acclimate or adapt to warming temperatures, sometimes with opposing effects. It is also important for accurately scaling species' functional responses to changing environments to ecosystem-level processes[17]. Here we used data fusion of high spatial resolution (~ 20 cm) unoccupied aerial vehicle (UAV) simultaneous measurements of thermal emissivity, optical reflectance, and LiDAR point cloud intensity of a 4-ha tropical montane wet forest plot on the Island of Hawai'i, and 10-min resolution climate data (air temperature, net radiation, wind speed, and vapor pressure deficit derived from temperature and relative humidity) from a climatological tower at the site to[1]: disentangle the effects of species' crown architectural traits on canopy temperatures (T_{can}) for the whole crown compared to only sunlit leaves[2], quantify within and among species' differences in T_{can}, and[3] compare the relative effects of biotic (crown traits) and abiotic factors on canopy temperature departures from air temperature (T_{diff}). Even small temperature differences among species should have large effects on metabolic and biophysical processes because of their nonlinear relationships with temperature[27].

In this study, we capture population-level variation of four co-occurring native Hawaiian tree species by mapping over 650 tree crowns in the Laupāhoehoe forest canopy. These species included koa (*Acacia koa*), 'ōlapa (*Cheirodendron trigynum*), pilo (*Coprosma rhynchocarpa*), and 'ōhi'a lehua (*Metrosideros polymorpha)* (Figs. 1 and 2), which is of current conservation concern due to the widespread invasive fungus (*Certatocystis spp.*) causing rapid 'ōhi'a death (known as "ROD") across multiple Hawaiian islands. Hawaiian forests generally host low species diversity compared to other tropical forests due to their isolation but are high in functional diversity[28] and have similar structure to other tropical forests[29]. For more details on the study location and data collection, please see materials and methods and Supplementary Figs. 1 and 2.

To discern how species' crown architecture differences (Fig. 1) affect T_{can} and T_{diff} of entire crowns vs. isolated sunlit leaves, we applied sequential filters to our thermal data (Fig. 2a) which allowed us to compare temperatures at both the crown-level and the leaf-level. For the crown-level analysis, which contains a mix of both sunlit and shaded leaves as well as non-photosynthetic vegetation, our data filtering first identified and separated pixels of dense vegetation biomass from pixels of sparse vegetation biomass and understory using LiDAR intensity data (Fig. 2a and Supplementary Fig. 3). For the leaf-level analysis, our data filtering involved two

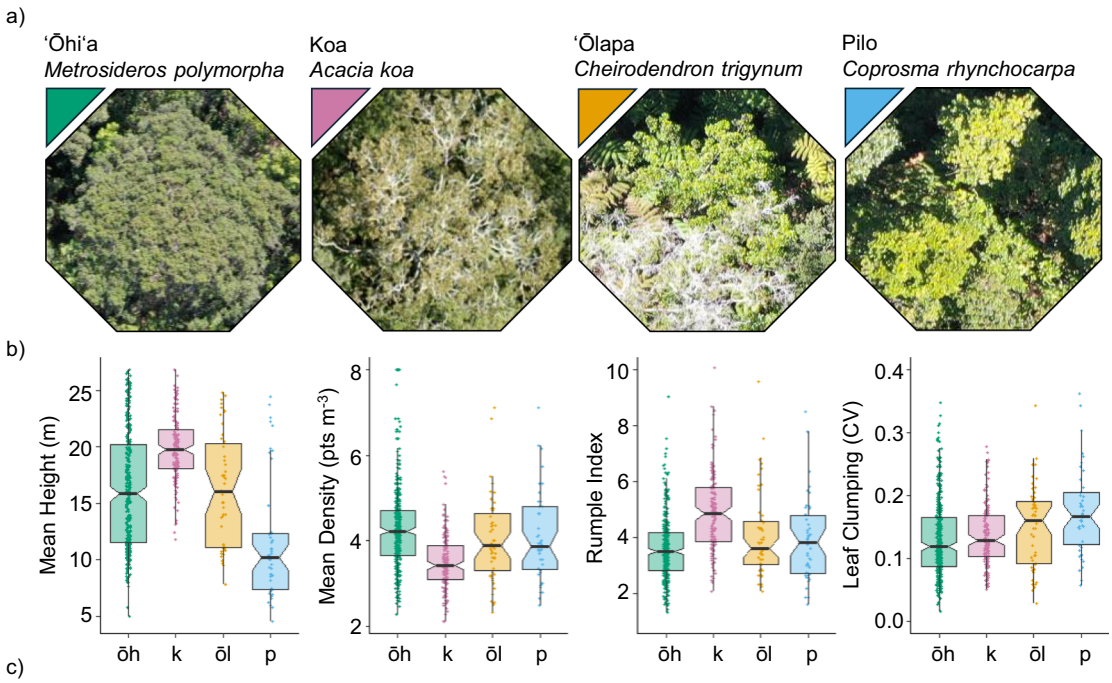

Fig. 1 | Forest canopy species' crown architecture traits, and hypotheses related to T_{can} and T_{diff}. a Images represent typical crowns (octagons) of each species, sampled from UAV-collected RGB imagery: 'Ōhi'a lehua *(Metrosideros polymorpha)* and Koa (*Acacia koa*) dominate the canopy at Laupāhoehoe forest plot (see distribution in forest crown map in Fig. 1 and field location in fig. S1). 'Ōlapa (*Cheirodendron trigynum*) and Pilo (*Coprosma rhynchocarpa*) are subdominants that also reach canopy heights. **b** Boxplots show species' (represented by color; ōh = 'ōhi'a, k = koa, ōl = 'ōlapa, p = pilo) differences in crown architectural traits derived from Lidar (~20 cm), from left to right: mean crown height (m), mean crown density (pts m^{-3}), crown rugosity (rumple index), and leaf clumping (CV). These are the same traits used in analyses of biotic and abiotic explainers of T_{diff}. The center line represents the median, the box edges represent the interquartile range, and the whiskers represent the variability in the upper and lower quartiles. **c** Hypotheses related to species' traits and crown temperatures (T_{can}), and crown temperature deviations from ambient air (T_{diff}).

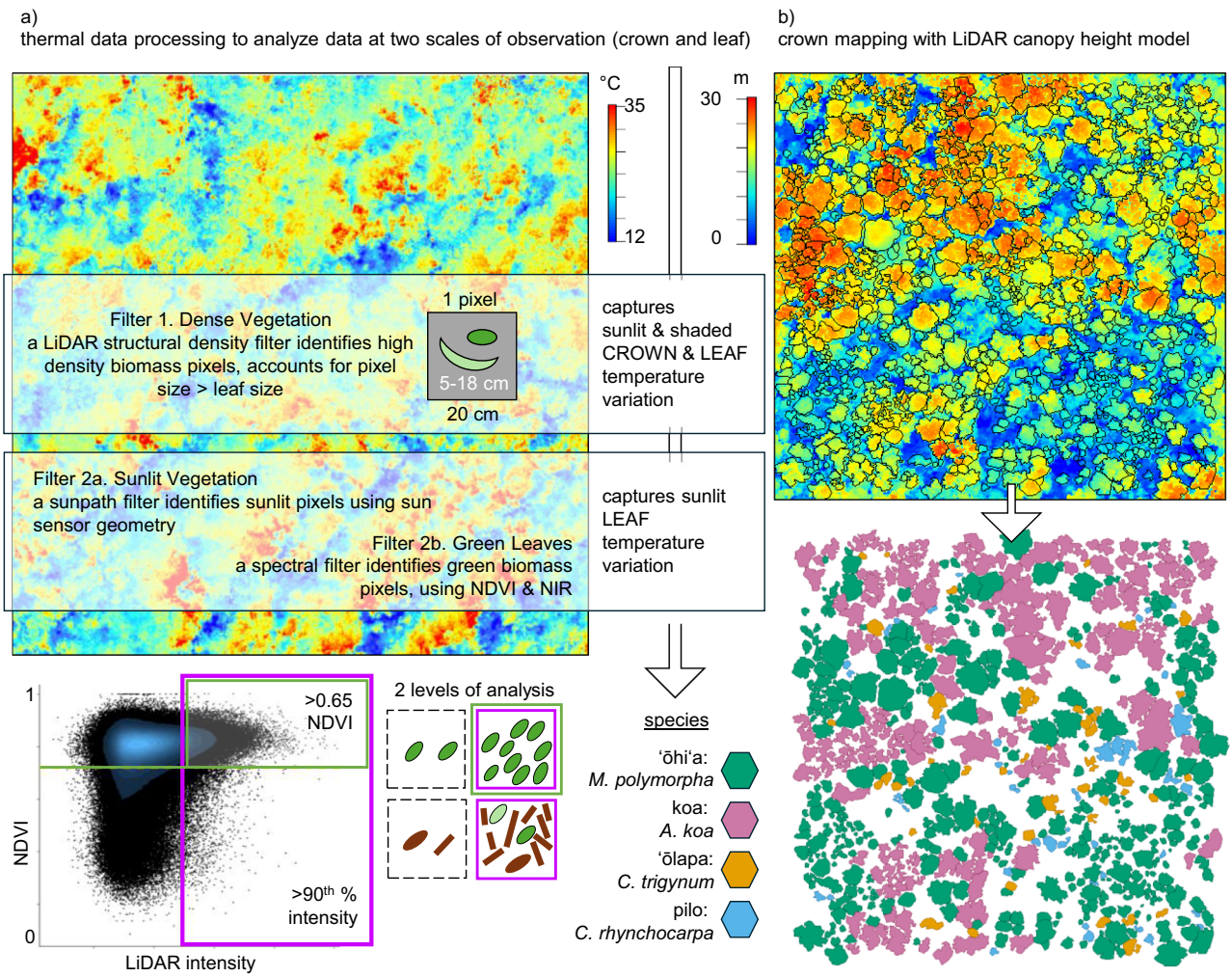

Fig. 2 | Data collection and filtering steps for observing canopy temperature at two levels of observation. a Map of canopy temperature from one flight (of five) over the 4-hectare Laupāhoehoe forest plot on the Island of Hawai'i. Five UAV flights collected thermal data across two days at 9:02, 10:18, and 10:48 am, and 1:01, 2:56 pm. Explanation of filtering steps to separate the effects of forest and crown physical structure on sunlit leaf temperatures. Analyses were repeated after each filter (1 and 2) at 2 levels of analysis[1]: crown-level: pixels with dense vegetation identified using LiDAR intensity values. Analysis at the crown-level includes pixels with high density photosynthetic and non-photosynthetic vegetation in the sun and shade and excludes pixels with sparse vegetation and understory; and[2] leaf-level: sunlit vegetation identified using sun sensor geometry and green photosynthetic vegetation (leaves) identified using spectral filters. Analysis at the leaf-level includes pixels with high density sunlit green leaves, excluding non-photosynthetic vegetation and shaded areas of the canopy. By isolating sunlit pixels with high green leaf density, cumulative filtering steps remove the effects of canopy and crown structure on crown temperatures to just represent the effects of sunlit leaves on observed temperatures. The scatterplot shows the relationship between LiDAR point intensity and the Normalized Difference Vegetation Index (NDVI) with each black point representing a single 20 cm^2 pixel. The purple box represents the structural LiDAR filter (filter 1) which identifies and removes pixels below the 90th percentile of LiDAR intensity values – pixels in which vegetation density is low. The horizontal green line represents the non-linear relationship between NDVI and canopy structure, where NDVI saturates around 0.65 (filter 2b), above which green standing biomass is captured. The green box highlights pixels retained after all filtering steps. **b** Top shows a LiDAR-derived canopy height model (CHM, scale in meters) used in combination with RGB imagery and tree census maps to outline tree crowns; Below shows each crown, as in the CHM, identified to species, represented by color. To analyze data, pixels remaining at each step of the filtering process were aggregated by crown and averaged to calculate T_{can}.

further steps. We separated sunlit from shaded dense vegetation pixels using sunpath geometry. Then, because dense vegetation pixels can contain non-photosynthetic vegetation such as portions of branches or brown leaves, we further identified green photosynthetic vegetation from all dense vegetative pixels using spectral greenness filters (Fig. 2a and Supplementary Fig. 4). After applying the data filters, we effectively eliminate the direct influence of crown architectural traits on crown temperature, isolating pixels within species-specific crowns that are sunlit green leaves before aggregating pixels to each mapped crown (Fig. 2b and Supplementary Fig. 5). At the crown-level, we hypothesize that species with higher crown density to be warmer, species with higher crown rugosity to be cooler, taller crowns to be cooler, and crowns with higher leaf clumping to be cooler. We also expect that these species' differences in T_{diff} will be scale-dependent due to potentially opposing effects of leaf and crown trait variation (e.g., a dense crown with small leaves vs. a sparse crown with large leaves could exhibit similar temperatures when observed at the crown-scale but diverge when observed at the leaf-scale). Though we do not directly measure leaf traits, we assume that leaves within the upper canopies of individual trees within species are comparable to each other, thus differences observed across scales (crown vs. leaf) can be attributed to crown architectural traits.

Results and discussion

Greater interspecific temperature differences at the leaf scale

We detected more *inter*specific differences at the leaf-scale after removing the influence of crown architecture (after filters 2a and 2b; Figs. 2a and 3a, b, Supplementary Fig. 6 and Supplementary Table 1). We also detected larger

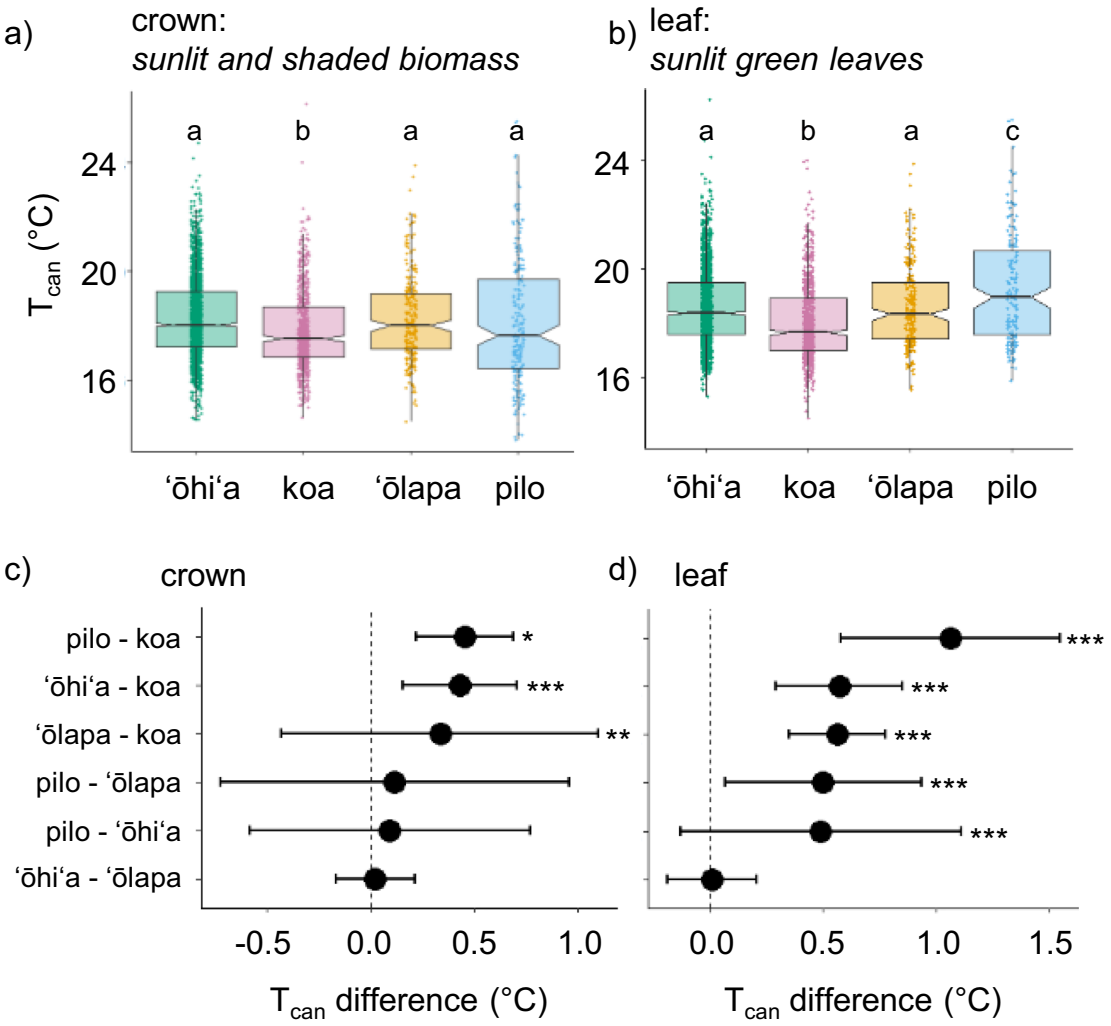

Fig. 3 | Species canopy temperature comparisons. Boxplots represent species crown temperatures in degrees Celsius (°C) across all five UAV flights for (**a**) sunlit and shaded dense biomass, "crown" and, (**b**) for sunlit green leaves, "leaf." In (**a**, **b**) each data point is an individual crown measurement. The center line represents the median, the box edges represent the interquartile range, and the whiskers represent the variability in the upper and lower quartiles. Letters denote statistically significant differences between species at $p < 0.05$. In (**c**, **d**) Points represent mean crown temperature differences in °C between species pairs across all five UAV flights (plus or minus 1 standard deviation) for "crown" (**c**) and "leaf" (**d**). In (**c**, **d**) statistically significant differences at $p < 0.05$ between species are denoted with asterisks.

relative differences between species (Fig. 3c, d). In other words, average crown temperature differences between species were larger at the leaf-scale (Fig. 3c, d). As examples, the average crown temperature difference between ʻōhiʻa *(M. polymorpha)* and koa *(A. koa)* grew from 0.44 °C (crown-level) to 0.59 °C (leaf-level) (Supplementary Table 1); and the average crown temperature difference between pilo *(C. rhynchocarpa)* and koa grew from 0.32 °C to 1.26 °C, respectively (Supplementary Table 1). These results suggest that interspecific variation may be more difficult to capture at the crown-level.

Focusing on the leaf-level, we found that sunlit ʻōhiʻa leaves (*M. polymorpha)* were consistently hotter than those of koa *(A. koa)* throughout the day (Fig. 3 and Supplementary Fig. 7), a species comparison especially important because ʻōhiʻa and koa dominate the canopy of many forests across the Hawaiian archipelago. At our study site, ~60% of the canopy (total number of crowns) comprised ʻōhiʻa crowns and ~24% of the canopy comprised koa crowns (Fig. 2b). On average, ʻōhiʻa leaf temperatures were 0.59 °C hotter than koa leaf temperatures (Fig. 3b, d), with differences at separate observation times ranging from 0.28–0.84 °C (Supplementary Fig. 7 and Supplementary Table 2). We had expected ʻōhiʻa temperatures to exceed those of koa because ʻōhiʻa leaves tend to be more directly oriented towards the sun, and in denser canopies than koa leaves (Fig. 1a), and because koa crowns are, on average, taller with higher rugosity than ʻōhiʻa crowns (Fig. 1b). However, the largest interspecific temperature difference at the leaf level was between pilo (*C. rhynchocarpa)* and koa, with pilo leaves 1.84 °C hotter than koa leaves in the afternoon (~ 1:00 p.m.; Supplementary Fig. 7 and Supplementary Table 2), and an average of 1.26 °C hotter across all observation times (Fig. 3b, d). Pilo leaves were significantly warmer than all other species, which was only apparent at the leaf-level. At the crown level, which includes the influence of crown architecture traits and the influence of those traits on the distribution of sun and shade leaves, pilo temperatures were cooler and closer to other species. These results align with a recent study that found observing whole-crown temperatures miss measuring the highest temperatures that leaves experience, which could lead to underestimating leaf heat stress near photosynthetic heat tolerance thresholds[12]. These high temperature hotspots also align with a strong right skew in the spatial distribution of hyperspectral vegetation indices across a forest canopy in Panama[30]. In our data all species show a right skew with hotspots of especially high temperatures, with pilo showing the least skewness and kurtosis (i.e., the most variation in temperatures across times of day and crowns) and koa showing the highest skewness and leptokurtosis (Supplementary Fig. 6a and Supplementary Table 3).

Trade-offs between leaf traits (e.g., size) and crown architectural traits (e.g., roughness) can have opposing effects crown temperatures. ʻŌhiʻa (*M. polymorpha)* and ʻōlapa (*C. trigynum)* were the only species that did not

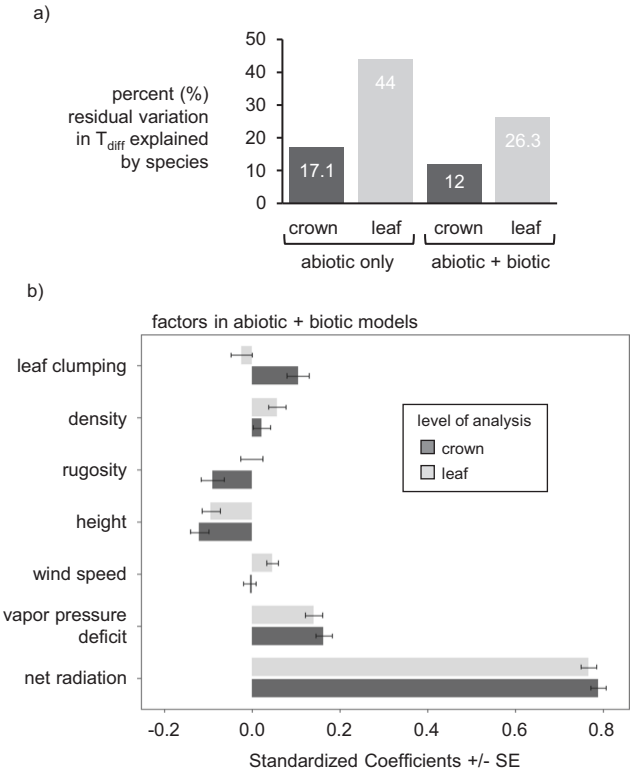

Fig. 4 | Accounting for crown architectural traits reveals different drivers of T_{diff} for sunlit green leaves. Linear mixed-effects models describe canopy variation in T_{diff} across all five UAV flights. All variables were standardized (z-transformed) prior to running the models. Species identity was included in the model as a random effect. **a** Bar plot represents the percentage (%) of residual variation in T_{diff} explained by species identity at the crown (sunlit and shaded dense vegetation; represented by darker grey bars) and leaf (sunlit green leaves; represented by lighter grey bars) level of analysis, and when only abiotic factors are included in models (leftmost two bars) vs. when abiotic and biotic factors are included in models (rightmost two bars). **b** Relative strength of biotic (leaf clumping, density, rugosity, height) and abiotic (wind speed, vapor pressure deficit, net radiation) predictors explaining forest T_{diff} at two levels of data analysis (crown and leaf, represented by darker grey and lighter grey, respectively, as in (**a**). Error bars denote the standard error around the estimates. The abiotic factors in the analysis vary across time while the biotic factors in the analysis vary across space (different tree crowns).

show significant differences in leaf temperatures (Fig. 3b, d and Supplementary Table 1) across all observations, or at any specific observation time of day (Supplementary Table 2). Though we did not directly measure leaf size in this study, ʻōlapa has larger leaves than ʻōhiʻa (see materials and methods), and rougher crowns with more leaf clumping (Fig. 1b). The larger leaves in ʻōlapa (large leaves tend to be warmer) may be counteracted by the roughness of their crowns (which facilitates heat loss through turbulent mixing with the surrounding air), while the smaller leaves in ʻōhiʻa (which tend to be cooler) may be counteracted by a smoother crown architecture (which can suppress turbulent mixing and maintain warmer crown temperatures). Such trade-offs can explain why, despite significant trait differences between the species, overall crown temperatures did not vary as much as leaf temperatures. Additionally, while leaves in full sun may thermoregulate differently due to differences in leaf physiology and morphology, accounting for inherent spatial heterogeneity within tree crowns can result in more similar temperatures because shaded leaves will have more similar temperatures (see further discussion of abiotic factors below).

Species have different intraspecific Tcan variance

Along with pairwise inter-specific average temperature differences discussed above (Fig. 3, Supplementary Figs. 6 and 7), species also exhibited different intra-specific differences in crown temperatures (Supplementary Fig. 6b). Species' crown temperature variances across the canopy were not homogeneous (Levene's Test for Equality of Variances: (a) at the crown-level, $F(3,3230) = 35.6$, $p < 0.001$; and (b) at the leaf-level, $F(3,2960) = 17.5$, $p < 0.001$) (Supplementary Fig. 6b, boxplot comparisons *across* species).

Only ʻōhiʻa *(M. polymorpha)* differed in intraspecific crown temperature variance across scales of observation (Supplementary Fig. 6b, boxplot comparisons of tree crowns within species across filter levels). ʻŌhiʻa showed different variance structure at the crown-level and the leaf-level (Levene's Test for Equality of Variances: T_{can}: $F(1,3824) = 5.4$, $p = 0.02$), suggesting that leaf-scale effects on T_{can} are less variable than effects from whole-crown traits (Supplementary Fig. 6b). Similarly, pilo *(C. rhynchocarpa)* appears to have highly variable temperatures when considering differences in crown architecture (i.e., highly variable crown architecture across the population), whereas isolating to the leaf-level results in much less variability, and similar variability to other species, in crown temperatures across the population (Supplementary Fig. 6b). These results reveal important interactions of leaf and whole-crown trait effects on moderating canopy temperatures and show that some species may have greater capacity (e.g., plasticity) to modify crown architecture as a thermoregulation trait.

Interspecific Tdiff variation across scales

The importance of species identity explaining T_{diff} (T_{can}-T_{air}) increased at the leaf-level (Fig. 4a), supporting the results described above that species' thermal differences associated with leaf-scale traits may be larger than those associated with whole-crown traits. When we included abiotic (net radiation, vapor pressure deficit, wind speed) and biotic (crown density, height, and rugosity) factors in models, species' identity explained 12.0% of the residual variation in T_{diff} at the crown-level (Fig. 4a). However, at the leaf-level, when examining only sun-lit, green photosynthetically active portions of crowns, the residual variation in T_{diff} explained by species identity increased to 26.3% (Fig. 4a and Supplementary Table 4). When biotic factors were not explicitly considered in these models, species' identity explained even more of the residual variation in T_{diff}: 17.1% (crown) and 44.0% (leaf) (Fig. 4a), presumably because differences in species' identity are related to crown traits. The species effect we identified suggest that tropical tree species differ considerably in their leaf thermal regulation strategies. Yet these divergent responses may be obscured at scales of observation that conflate leaf morphological and physiological and crown-architectural influences on canopy temperatures.

Abiotic and biotic drivers of Tdiff across scale

For the entire Laupāhoehoe forest canopy, at both levels of analysis (crown and leaf, respectively) we found that net radiation was the strongest predictor of T_{diff} (standardized parameter estimate = $0.79 +/- 0.02$ and $0.77 +/- 0.02$), compared to the other two abiotic drivers considered, vapor pressure deficit (VPD; $0.16 +/- 0.02$ and $0.16 +/- 0.02$) and wind speed ($0.00 +/- 0.01$ and $0.05 +/- 0.01$) (Supplementary Table 4). This aligns with previous evidence from a tropical forest, which showed the importance of net radiation in tropical forests relative to VPD and wind speed[13]. Of the biotic predictors, we found that tree height was the strongest predictor of T_{diff} at both levels of analysis, with taller tree crowns experiencing temperatures closer to air temperature (lower T_{diff}). However, this effect of tree height was stronger at the leaf-level (standardized parameter estimate = $-0.12 +/- 0.01$) than at the crown-level of analysis ($-0.09 +/- 0.02$; Fig. 4b and Supplementary Table 4). Crown rugosity had a stronger effect on T_{diff} than crown density at the crown-level (note, crown traits were measured on tree crowns *prior* to applying the first data filter; Fig. 2a). Though having the opposite effect, leaf clumping was comparable to the strength of the effect of tree height at the crown-level but was less important at the leaf-level (Fig. 4b and Supplementary Table 4). Crown density had very little effect on T_{diff} at either level of analysis (Fig. 4b and Supplementary Table 4). In other words, it is perhaps not total leaf area, or density, contributing to T_{diff}, but how that leaf area is distributed and exposed to sunlight or shade within the tree canopy.

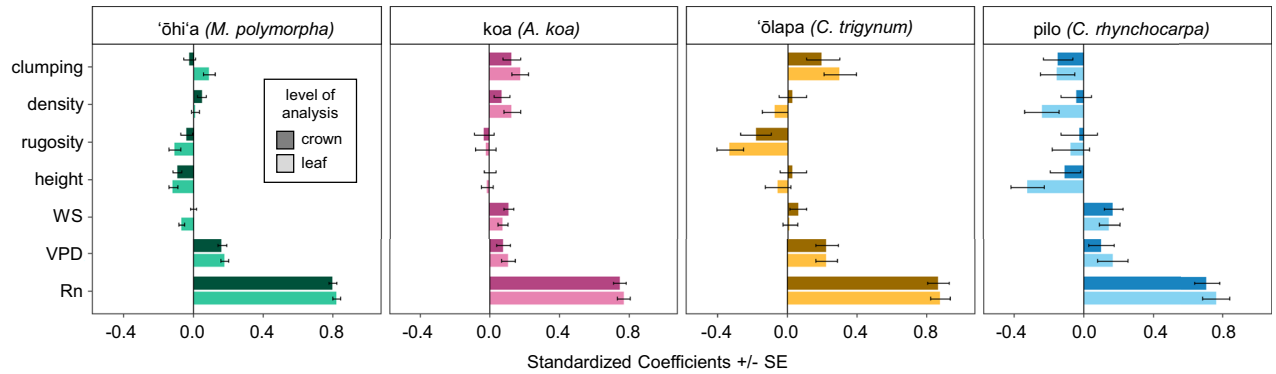

Fig. 5 | Bar plots represent the results of linear models split by species. Strength of biotic (leaf clumping, crown density, crown rugosity, crown height) and abiotic (wind speed (WS), vapor pressure deficit (VPD), net radiation (Rn)) predictors explaining T_{diff} at two levels of data analysis (crown and leaf, represented by darker and lighter shades of color, respectively). "Crown" refers to sunlit and shaded dense vegetation, while "leaf" refers to only sunlit green leaves. All predictors were standardized (z-transformed). Error bars denote the standard error around the estimates. The abiotic factors in the analysis vary across time while the biotic factors in the analysis vary across space (different tree crowns).

Though net radiation in our data remained the strongest predictor across scales and for all species (Fig. 5), applying the same model after each level of filtering revealed scale-dependent, species-specific interactions (Supplementary Table 4). Because species identity explained a high percentage of the residual variation in T_{diff} after isolating leaf-scale differences (26.3%; Fig. 4a and Supplementary Table 4), we evaluated the thermal data by species and for each, we again tested the relative effects of abiotic and biotic factors on T_{diff} (Fig. 5 and Supplementary Table 5). The relative effect of net radiation ranged from 0.71 (*C. rhynchocarpa*, crown-level) to 0.88 (*C. trigynum*, leaf-level); the effect of VPD was more wide-ranging across species, from 0.08 (*A. koa*, crown-level) to 0.23 (*C. trigynum*, crown and leaf-level); and the effect of wind speed ranged from 0.00 (*M. polymorpha*, crown-level) to 0.17 (*C. rhynchocarpa*, crown-level) and was not a significant predictor of T_{diff} for *M. polymorpha* at the crown-level or *C. trigynum* at the leaf- and crown-level (Fig. 5 and Supplementary Table 4). These differences at varying scales emphasize how co-occurring species may diverge in their responses to the same ambient conditions. Specifically, the trends reveal an important interaction between abiotic conditions and crown thermal dynamics at different scales of observation. Net radiation and VPD are strongly tied to physiological leaf-scale processes like stomatal behavior[23,31], which we expected to become stronger predictors when leaf-scale effects were not conflated with crown architecture, however, it was wind speed, which interacts with crown architecture and 3-dimensional structural properties of forests such as boundary layer conditions and the degree of turbulent mixing[15,26], that had a stronger overall effect in the forest canopy after isolating leaf-scale differences (Fig. 4b).

The intra- and inter-specific variation in tree crown traits of each species (i.e., height, density, rugosity, leaf clumping; Fig. 1b) do have species-specific effects on T_{diff}. For instance, though ʻōhiʻa (*M. polymorpha)* has the highest crown density (Fig. 1b), density had a small effect on T_{diff} at the crown-level and, counter to expectations, had no meaningful effect on T_{diff} at the crown-level for the other three species (Fig. 5 and Supplementary Table 5). Crown density had a positive effect on koa *(A. koa)* T_{diff} at only the leaf-level, and a negative effect for pilo *(C. rhynchocarpa)* at the leaf-level (Fig. 5 and Supplementary Table 5). At the crown-level, height only had a significant negative effect on T_{diff} for ʻōhiʻa, and at the leaf-level height only mattered for ʻōhiʻa and pilo, with a particularly strong effect for pilo (Fig. 5 and Supplementary Table 5). Crown rugosity (rumple index) was only important for ʻōlapa *(C. trigynum)* at both levels of observation, and for ʻōhiʻa at the leaf-level of observation (Fig. 5 and Supplementary Table 5), having a negative effect on T_{diff}. Finally, leaf clumping had a significant positive effect (increasing T_{diff}) for koa and ʻōlapa at the crown-level and leaf-level and for ʻōhiʻa at the leaf-level (Fig. 5 and Supplementary Table 5). It should be noted that crown density and crown rugosity were correlated for all species (correlation coefficients between −0.7 and −0.82, depending on species; Supplementary Fig. 8).

Our findings identify scale-dependent effects on crown and canopy responses to environmental drivers. We expected that species experiencing the same ambient temperatures would differ in crown temperatures, and that species' differences in T_{diff} would be scale-dependent due to crown and leaf trait variation interacting with abiotic conditions (Fig. 1c). We found nuanced scale-dependent interactions between ambient abiotic conditions and species traits in (a) species' T_{can} differences (Fig. 3 and Supplementary Table 5), and (b) variation in the strength of biotic and abiotic drivers on species' T_{diff} (e.g., Fig. 5 and Supplementary Table 5). The differences we observed (leaf- to whole-crown; Fig. 3, Fig.5, and Supplementary Table 2) emphasize why we must consider processes occurring at different scales to understand species' responses to warming temperatures.

Trees may acclimate or adapt to warming temperatures by modifying a suite of leaf and crown traits. These trait responses, if just observed at a crown-level, may be confounded if leaf traits strongly respond to one environmental driver while crown architecture traits respond to another. The endemic ʻōhiʻa lehua *(Metrosideros polymorpha)* is a foundational species across the entire Hawaiian archipelago[32]. Because of the steep climatic and substrate-age gradients across the islands' forests, ʻōhiʻa is well-known to present high intraspecific variation in leaf and whole-plant phenotypes and to be locally adapted in many parts of its range, tolerating a wide variety of environmental conditions. Thus, the species may have a high adaptive capacity along to respond to future shifts to temperature[33–37], although in our data ʻōhiʻa did not exhibit more intraspecific variation in T_{crown} compared to other species (Supplementary Fig. 6). Differences in crown traits (e.g., Fig. 1b) between ʻōhiʻa and koa, and leaf trait differences (e.g., stomatal conductance; 38-41) have implications for leaf temperature regulation and can help explain temperature differences between the species. Koa, typically found in wet habitats, exhibits higher and more variable stomatal conductance[38,39] than ʻōhiʻa, a species that can be found across a range of dry to wet environments. This means koa has the potential for higher gas exchange and water vapor release, and therefore more effective transpirational cooling of koa leaves. In contrast, ʻōhiʻa exhibits a lower and less variable stomatal conductance[40,41], aligning with a more conservative water-use strategy and a comparatively lower ability to respond. This contrast could help explain the patterns we see of koa leaves being cooler than ohia leaves (e.g., Fig. 3b). leading to hotter leaf temperatures. Possible opposing responses to environmental drivers at different scales of observation (and levels of trait variation), could obscure our understanding of how these species and forests are thermoregulating in response to a changing climate.

Analyzing patterns and processes across multiple scales of observation is critical because observed patterns at one scale may be driven by processes occurring at other scales[42]. For instance, observations of thermal stress at the crown scale could be from physiological processes breaking down at the leaf scale and/or from structural changes like leaf abscission at the crown-scale. Spatially-explicit analyses of thermal imagery can be used not only to measure canopy-scale thermal variation across forested landscapes[17,19] but also to capture processes occurring at the leaf and crown scales of individual trees (e.g., Figs. 1–5). The filtering approach we developed can help disentangle whether changes in individual tree crowns and across species, in response to environmental change (e.g., drought sensitivities, 18), are likely driven by structural change or physiological responses. This distinction is especially important to make within tropical forests that are "green year-round"—a characteristic that makes it difficult to resolve species' unique phenological patterns that have significant effects on carbon cycling and other ecosystem functions[43–45]. Because most remote sensing and thermal imaging analysis occurs at scales that conflate effects driven by processes at different scales, we may be significantly confounding heterogeneous responses of forests to climate change. In studying the thermal dynamics of forests, our work shows the importance of considering multiple scales of observation, understanding inter- and intra-specific variation in traits, and the scale-dependent nature of species' responses to climate change.

Tropical species may be sensitive to warming temperatures due to their evolution in stable climates[1], making it important to understand how unique species traits, both physiological and structural, influence their responses to climate change. Our results show the importance of species' identity and species-specific traits in explaining how much crown temperatures deviated from air temperatures, and that these species differences were dampened at the crown compared to leaf level. We show that leaf-level temperatures may overestimate whole-crown temperatures due to the temperature-modulating effects of crown architecture, which has implications for scaling leaf temperatures to land surface temperatures. Conversely, focusing only on whole-crown temperatures may underestimate the heat stress being experienced by sunlit leaves, leading to an incomplete understanding of whether leaf temperatures are nearing photosynthetic heat tolerance thresholds[12]. Modifying crown architecture traits, often overlooked compared to leaf traits, is one way species can adapt or acclimate to warming temperatures, highlighting the many ways that species can uniquely respond to global change.

Materials and methods

Site Information

The field site at Laupāhoehoe, HI (lat, long: 19.930, -155.29) is a 4-hectare plot, which is part of the Hawai'i Permanent Plot Network (HIPPNET; described in detail in 29), and the Smithsonian ForestGEO Network (The Center for Tropical Forest Science and Forest Global Earth Observatories CTFS-ForestGEO). The plot exists at approximately 1155 to 1170 m in elevation off the windward eastern coast of Hawai'i island (Supplementary Fig. 1). The Laupāhoehoe site is a montane wet forest comprised of 18 flowering plants and a canopy dominated by 'ōhi'a lehua (*Metrosideros polymorpha*) and koa (*Acacia koa*) (Fig. 1). Forests dominated by 'ōhi'a, or a mix of 'ōhi'a and koa, represent 38% of the total forest cover on the island of Hawai'i[46], and both species are of cultural significance to Hawaiians. Further, 'ōhi'a is of conservation concern due to the widespread invasive fungus (*Certatocystis spp*.) causing rapid 'ōhi'a death (ROD) on at least three of the Hawaiian Islands (Hawai'i, Oahu, and Kaua'i). Other trees that reach canopy or sub-canopy height include pilo (*Coprosma rhynchocarpa*) and 'ōlapa (*Cheirodendron trigynum*) (Fig. 1). Though we did not measure leaf traits directly in this study, the species vary in leaf traits such as size, shape, thickness, and orientation. For example, koa has curved, narrowly lance-shaped leaves, 10–15 cm long and 6–25 mm wide; 'ōhi'a has crowded, opposite leaves that are elliptical or ovate, 2–7.5 cm long and 1.3–4 cm wide; 'ōlapa has large rounded leaves 5–18 cm long, with widths reaching almost half the length; pilo has leaves that are about 5.5–15 cm long and 2–5 cm wide[47,48]. It was estimated (2008–2013) that the site holds between 366–464 Mg ha^{-1} of aboveground biomass and 11–13.6 Mg ha^{-1} yr^{-1} of aboveground wood production; the mean annual temperature at this site is 16 °C, and the mean annual precipitation is 3440 mm[49].

UAV data collection

Data were collected on March 7 and March 11, 2022, and flights began at 9:02 am, 10:18 am, 10:48 am, 1:01 pm, and 2:56 pm, spanning 15-20 minutes each. The GatorEye sensor suite flew 120 meters above ground level and at ten m s^{-1} speed. The sensors were a VLP32c lidar sensor, a6000 visual camera, custom Phoenix Aerial radiometric thermal camera with lab calibrations and temperature stabilization shell, and a Headwall Photonics Nano hyperspectral camera. The Phoenix LiDAR Systems PT640 thermal camera uses a custom calibrator to improve temperature accuracy. Every ten seconds, instead of capturing the area of interest (canopy), the camera captures an image of a uniformly heated plate blackbody within the camera housing to perform an external dark-frame non-uniformity correction. This adjustment prevents thermal drift from occurring as it makes measurements across the data acquisition period. We assumed a constant vegetation emissivity value of 0.95[7]. The hyperspectral camera captures spectral bands from the visible spectrum through the short-wave infrared region (wavelengths range from 400–1000 nm). Orthomosaics with a 20 cm^2 pixel resolution were created for RGB, Thermal (°C), and lidar intensity with detailed methods and calibration information described in ([50,51], and available at www.gatoreye.org).

Tree crown delineation

Tree crowns were delineated in ArcMap (version 10.7.1[52];) from orthomosaiced RGB imagery obtained in March 2022 (Supplementary Fig. 1). This was an iterative process by which confidence in the species identification and in the polygons were remarked until as many crowns as possible were designated with qualitatively "high confidence." Crowns marked with lower confidences were revisited with individual high-resolution drone images to identify the species and align with a georeferenced census dataset of individual stem locations. Any crowns that remained categorized as "low confidence" after careful and repeat inspection were left out of final analyses. We "rasterized" the tree crown polygons in R (version 4.1.3[53];) to match the spatial resolution and extent of the thermal data. All analyses were conducted with averages of the pixels within each crown. Primarily for *Acacia koa*, a single identified crown may be a large leaf cluster (i.e., a portion of a single crown), as it was difficult to determine which individual a leaf cluster belonged in areas with many separate *A. koa* stems. This may have artificially increased the sample size for *A. koa* but should not affect our primary results and conclusions. Our process resulted in a total of 652 crowns or leaf clusters split between the four species: 396 *Metrosideros polymorpha* ('ōhi'a lehua), 159 *Acacia koa* (koa), 51 *Cheirodendron trigynum* ('ōlapa), and 46 *Coprosma rhynchocarpa* (pilo) crowns or leaf clusters. The exact numbers of crowns included in each analysis varied by time of day and filtering level (see details below and in Supplementary Tables 1 and 2).

Tree crown traits

For each delineated tree crown, we extracted average height (m) from the canopy height model depicted in Fig. 2B. We also calculated the coefficient of variation (CV) of crown height (the ratio of standard deviation to mean height) within each crown as a measure of leaf clumping that is comparable across crowns of different mean heights. Higher CV indicates a more uneven, "clumped" distribution of canopy heights and greater structural variability within the crown. With the R package "lidR"[53–55], we used the function "voxel_metrics" to derive average crown densities (pts m^{-3}) from 3D point densities from Lidar point clouds and the function "rumple_index" to calculate the rumple index (a measure of rugosity or roughness) for each crown. Higher rumple index values indicate more uneven, or rough, canopy structure[55].

Filtering thermal data to account for structure and physiology

To analyze responses of well-lit and leafy vegetation pixels, we filtered thermal data prior to analyses. Thermal data were processed through the following consecutive filters[1]: a LiDAR intensity filter, and[2] a sunpath and a spectral filter (Fig. 2). The goal of these filters was to isolate the sunlit leaf-level effects on canopy temperatures by removing the impact of crown structure (e.g., crown density, non-photosynthetic versus photosynthetic vegetation), and sun angle. The first filter applied to the thermal data was a mask of LiDAR intensity values above the 90th percentile at each observation (flight) time. LiDAR intensity is independent of the amount of sunlight hitting the canopy surface and provides insight into the leaf area density and angle distribution and the three-dimensional structure within forests, vegetation characteristics, and understory or terrain attributes. For example, the intensity of LiDAR return signals can reflect the density or sparsity of leaves or other biomass on tree crowns. This filter is also important because pixel size is larger than leaf size—ensuring that we analyze pixels within tree crowns that are primarily 'full' of objects, or vegetation. Though we may lose pixels with sparse leaves, a lower LiDAR threshold would capture sparser regions of the canopy and likely widen the temperature differences we find between leaves and crowns, especially for species with more open canopies. The next two filters were a sun path filter, which uses solar ray tracing and removes self-shaded leaves from our analysis, and a spectral filter, which allowed us to keep thermal data that corresponded to pixels with an NDVI (normalized difference vegetation index[56,57];) higher than 0.65 (where NDVI saturates) and a mean near-infrared reflectance (NIR, 770–800 nm) higher than 0.2[58]. The goal of these filters was to isolate high-intensity (high-density) pixels that are primarily green leaves from those pixels that are densely filled with non-green biomass such as branches or non-photosynthesizing leaves (Fig. 2).

Climate data

Climate data were collected from the climatological station at Laupāhoehoe Forest. We used air temperature, wind speed, relative humidity, upwelling, and downwelling short and longwave radiation data that were collected once every 10 minutes throughout the day. Because flight times took approximately 15–20 minutes each, we averaged the three data points closest to each flight time for our analyses. For example, for the first flight time (9:02 am), we used the average of data points collected at 9:00, 9:10, and 9:20 am.

From these averages of relative humidity and air temperature, we calculated vapor pressure deficit (VPD)—the amount of water in the air relative to the maximum amount of water the air can hold at a given temperature. We calculated VPD for the site at each flight time as:

$$\mathrm{VPD} = e_{sat} - e_a \quad (1)$$

where,

$$e_{sat}(\text{saturation vapor pressure}) = 6.112 \times \exp(17.67 \times T_{air})/(T_{air} + 243.5)(\text{mbar}) \quad (2)$$

$$e_{sat} = e_{sat} \times 100\left(\text{convert mbar to Pa} : (100\text{Pambar}^{-1})\right) \quad (3)$$

$$e_a(\text{ambient vapor pressure}) = e_{sat} \times \mathrm{RH100} \quad (4)$$

We also calculated net radiation (Rn)—the difference between incoming (downwelling) and outgoing (upwelling) radiation for the site at each flight time. This was calculated from 30-min averages of downwelling and upwelling shortwave radiation (SW_{down} and SW_{up}, respectively) and downwelling and upwelling longwave radiation (LW_{down} and LW_{up}, respectively):

$$R_n = SW_{down} - SW_{up} + LW_{down} - LW_{up} \quad (5)$$

The average daily temperature on March 7, 2022, was 14.7 °C, with temperatures ranging from 11.2-19.1 °C, and the average temperature on March 11, 2022, was 16.8 °C, ranging from 13.9–19.9 °C. No rainfall was recorded on either day. The 30-minute average conditions used in analyses at each of the five flight times are represented in Supplementary Fig. 2. Though soil water content (SWC) can be an important determinant of plant thermal regulation[13], it did not vary significantly across observations and was thus not included in the analysis of the abiotic drivers of T_{diff}.

Species canopy temperature differences analysis

We ran a linear model with species predicting T_{diff} to examine species differences. We used a post-hoc multiple comparison test (TukeyHSD function in base R; 53) at a confidence level of 0.95 and *p*-values to determine statistically significant differences in T_{diff} between species. We repeated this analysis at each level of analysis (crown and leaf) in the thermal data filtering process (Fig. 2a), and for each observation (flight).

Abiotic and biotic drivers of T_{diff} analysis

To assess the relative importance of different environmental conditions and crown traits on T_{diff}, we analyzed which factors explained more variation in T_{diff} using linear mixed-effects models in R[53] with the package "lme4"[59]. We included net radiation (Rn), vapor pressure deficit (VPD), and windspeed (WS) as fixed abiotic effects the model, crown density, rugosity (rumple index), crown height, and leaf clumping as fixed biotic effects in the model, and species identity as a random effect. All variables were standardized (z-transformed; centered and scaled) prior to running models to compare the relative strength of parameter estimates. The random effect of species identity was evaluated as the percentage of the residual variation explained. We repeated this analysis at both levels of analysis (crown- and leaf-level; Fig. 2a), and both with and without including the four biotic crown traits (Fig. 4a).

Within-species canopy temperature variation analysis

To test whether the variances in T_{can} between species were equal, and whether the variances in T_{can} between filtering steps within a species were equal, we used Levene's Test for Equality of Variance with the function "leveneTest" in the R package "car"[53,60]. If *p*-values were less than 0.05, we rejected the null hypothesis that the groups we were examining (species, filter levels) showed equal variances in T_{can}. We also assessed temperature distribution characteristics across species and levels of analysis (crown and leaf) by calculating the skewness and kurtosis using the R package "moments"[53,61]. We assessed normality with Anderson-Darling and Kolmogorov-Smirnov tests using the R package "nortest"[53,62]. These results are presented in Supplementary Table 3.

Reporting summary

Further information on research design is available in the Nature Portfolio Reporting Summary linked to this article.

Data availability

Data for this manuscript is available on Dryad at https://doi.org/10.5061/dryad.kwh70rzfp[63].

Code availability

All analyses were performed with publicly available R[53] packages (version 4.1.3; https://www.R-project.org/)[53]. Code for this analysis is available on GitHub (https://github.com/shanljbay/hawaii_crown_traits_and_temperatures.git).

Received: 26 July 2024; Accepted: 13 January 2025;
Published online: 18 January 2025

References

1. Wright, S. J., Muller-Landau, H. C. & Schipper, J. The Future of Tropical Species on a Warmer Planet. *Conservation Biology* **23**, 1418–1426 (2009).

2. Doughty, C. E. et al. Tropical Forests are approaching critical temperature thresholds. *Nature* **621**, 105–111 (2023).
3. K. Feeley. et al. The Thermal Tolerances, Distributions, and Performances of Tropical Montane Tree Species. *Front. Forests Glob. Change* **3**, https://doi.org/10.3389/ffgc.2020.00025 (2020).
4. Sullivan, M. J. P. et al. Long-term thermal sensitivity of Earth's tropical forests. *Science* **368**, 869–874 (2020).
5. Still, C. J. et al. No evidence of canopy-scale leaf thermoregulation to cool leaves below air temperature across a range of forest ecosystems. *PNAS* **119**, e2205682119 (2022).
6. Daughty, C. E. & Goulden, M. L. Are tropical forests near a high temperature threshold? *Journal of Geophysical Research* **113**, G00B07 (2008).
7. Aubrecht, D. M. et al. Continuous, long-term, high-frequency thermal imaging of vegetation: Uncertainties and recommended best practices. *Agricultural and Forest Meteorology* **228–229**, 315–326 (2016).
8. Rey-Sánchez, A. C., Slot, M., Posada, J. M. & Kitajima, K. Spatial and seasonal variation in leaf temperature within the canopy of a tropical forest. *Climate Research* **71**, 75–89 (2016).
9. Fauset, S. et al. Differences in leaf thermoregulation and water use strategies between three co-occurring Atlantic forest tree species. *Plant, Cell & Environment* **41**, 1618–1631 (2018).
10. Blonder, B., Escobar, S., Kapas, R. E. & Michaletz, S. T. Low predictability of energy balance traits and leaf temperature metrics in desert, montane and alpine plant communities. *Functional Ecology* **34**, 1882–1897 (2020).
11. Crous, K. Y. et al. Similar patterns of leaf temperatures and thermal acclimation to warming in temperate and tropical tree canopies. *Tree Physiology* **43**, 1383–1399 (2023).
12. O. J. L. Manzi. et al., Canopy temperatures strongly overestimate leaf thermal safety margins of tropical trees. *New Phytol.* **243**, 2115-2129.
13. Körner, C. & Hiltbrunner, E. The 90 ways to describe plant temperature. *Perspectives in Plant Ecology, Evolution, and Systematics* **30**, 16–21 (2018).
14. Still, C. J. et al. Imaging canopy temperature: shedding (thermal) light on ecosystem processes. *New Phytologist* **230**, 1746–1753 (2021).
15. R. Monson, D. Baldocchi. Terrestrial biosphere-atmosphere fluxes. (Cambridge, UL, Cambridge University Press, 2014).
16. Leuzinger, S. & Körner, C. Tree species diversity affects canopy leaf temperatures in a mature temperate forest. *Agricultural and Forest Meteorology* **146**, 29–37 (2007).
17. Farella, M. M., Fisher, J. B., Jiao, W., Key, K. B. & Barnes, M. L. Thermal remote sensing for plant ecology from leaf to globe. *Journal of Ecology* **110**, 1996–2014 (2022).
18. Scherrer, D., Bader, M. K. & Körner, C. Drought-sensitivity ranking of deciduous tree species based on thermal imaging of forest canopies. *Agricultural and Forest Meteorology* **151**, 1632–1640 (2011).
19. P. J. Olsoy. et al. High-resolution thermal imagery reveals how interactions between crown structure and genetics shape plant temperature. *Remote Sens. Ecol. Conserv.* https://doi.org/10.1002/rse2.359 (2023).
20. K. Yi. et al. High Heterogeneity in Canopy Temperature Among Co-occurring Tree Species in a Temperate Forest. *J. Geophys. Res. Biogeosci.* **125**, e2020JG005892.
21. Leuzinger, S., Vogt, R. & Körner, C. Tree surface temperature in an urban environment. *Agricultural and Forest Meteorology* **150**, 56–62 (2010).
22. A. Zakrzewska, D. Kopeć, K. Krajewski, J. Charyton, Canopy temperatures of selected tree species growing in the forest and outside the forest using aerial thermal infrared (3.6-4.9 μm) data. *Eur. J. Remote Sensing* **55**, 313-325.
23. Leigh, A. et al. Do thick leaves avoid thermal damage in critically low wind speeds? *New Phytologist* **194**, 477–487 (2012).
24. Leigh, A., Sevanto, S., Close, J. D. & Nicotra, A. B. The influence of leaf size and shape on leaf thermal dynamics: does theory hold up under natural conditions? *Plant, Cell & Environment* **40**, 237–248 (2017).
25. Slot, M. et al. Leaf heat tolerance of 147 tropical forest species varies with elevation and leaf functional traits, but not with phylogeny. *Plant, Cell & Environment* **44**, 2414–2427 (2021).
26. McNeil, B. E. et al. Tree crown economics. *Frontiers in Ecology and the Environment* **21**, 40–48 (2023).
27. Brown, J. H., Gillooly, J. F., Allen, A. P., Savage, V. M. & West, G. B. Toward a metabolic theory of ecology. *Ecology* **85**, 1771–1789 (2004).
28. Medeiros, C. D. et al. An extensive suite of functional traits distinguishes Hawaiian wet and dry forests and enables prediction of species vital rates. *Functional Ecology* **33**, 712–734 (2018).
29. Ostertag, R., Inman-Narahari, F., Cordell, S., Giardina, C. P. & Sack, L. Forest Structure in Low-Diversity Tropical Forests: A Study of Hawaiian Wet and Dry Forests. *PLoS ONE* **9**, e103268 (2014).
30. Merrick, T. et al. Unveiling spatial and temporal heterogeneity of a tropical forest canopy using high-resolution NIRv, FCVI, and NIRvrad from UAS observations. *Biogeosciences* **18**, 6077–6091 (2021).
31. Drake, J. E. et al. Trees tolerate an extreme heatwave via sustained transpirational cooling and increased leaf thermal tolerance. *Global Change Biology* **24**, 2390–2402 (2018).
32. Craven, D. et al. OpenNahele: The open Hawaiian forest plot database. *Biodiversity Data Journal* **6**, e28406 (2018).
33. Cordell, S., Goldstein, G., Melcher, P. J. & Meinzer, F. C. Photosynthesis and Freezing Avoidance in Ohia (Metrosideros polymorpha) at Treeline in Hawaii. *Arctic, Antarctic, and Alpine Research* **32**, 381–387 (2000).
34. James, S. A., Puttock, C. F., Cordell, S. & Adams, R. P. Morphological and genetic variation within Metrosideros polymorpha (Myrtaceae) on Hawaii. *New Zealand Journal of Botany* **42**, 263–270 (2003).
35. Sur, G. L., Keating, R., Snow, N. & Stacy, E. A. Leaf micromorphology aids taxonomic delineation within the hypervariable genus *Metrosideros* (Myrtaceae) on O'ahu. *Pacific Science* **72**, 345–361 (2018).
36. Ekar, J. M., Price, D. K., Johson, M. A. & Stacy, E. A. Varieties of the highly dispersible and hypervariable tree, Metrosideros polymorpha, differ in response to mechanical stress and light across a sharp ecotone. *American Journal of Botany* **106**, 1106–1115 (2019).
37. Barton, K. E. et al. Hawai'i forest review: Synthesizing the ecology, evolution, and conservation of a model system. *Perspectives in Plant Ecology, Evolution and Systematics* **52**, 125631 (2021).
38. Meinzer, F. C., Fownes, J. H. & Harrington, R. A. Growth indices and stomatal control of transpiration in *Acacia koa* stands planted at different densities. *Tree Physiology* **16**, 607–615 (1996).
39. Ares, A. & Fownes, J. H. Water supply regulates structure, productivity, and water use efficiency of *Acacia koa* forest in Hawaii. *Oecologia* **121**, 458–466 (1999).
40. Cordell, S., Goldstein, G., Mueller-Dombois, D., Webb, D. & Vitousek, P. M. Physiological and morphological variation in *Metrosideros polymorpha*, a dominant Hawaiian tree species, along an altitudinal gradient: the role of phenotypic plasticity. *Oecologia* **113**, 188–196 (1998).
41. Cornwell, W. K., Bhaskar, R., Sack, L., Cordell, S. & Lunch, C. K. Adjustment of structure and function of Hawaiian *Metrosideros polymorpha* at high vs. low precipitation. *Functional Ecology* **21**, 1063–1071 (2007).
42. Levin, S. A. The problem of pattern and scale in ecology. *Ecology* **73**, 1943–1967 (1992).
43. Pau, S., Detto, M., Kim, Y. & Still, C. J. Tropical forest temperature thresholds for primary productivity. *Ecosphere* **9**, e02311 (2018).
44. Piao, S. et al. Plant phenology and global climate change: Current progresses and challenges. *Global Change Biology* **25**, 1922–1940 (2019).

45. Sakai, S. & Kitajima, K. Tropical phenology: Recent advances and perspectives. *Ecological Research* **34**, 50–54 (2019).
46. Asner, G. P. et al. High-resolution carbon mapping on the million-hectare Island of Hawaii. *Frontiers in Ecology and the Environment* **9**, 434–439 (2011).
47. Harold L. Lyon Arboretum, University of Hawaii at Mānoa. *Plant Collections*. Harold L. Lyon A. https://www.hawaii.edu/arboretum (2024).
48. Little, E. L., Jr & Skolmen, R. G. (1989), *Common forest trees of Hawaii (native and introduced)* (Agricultural Handbook No. 679). U.S. Department of Agriculture, Forest Service.
49. Piponiot, C. et al. Distribution of biomass dynamics in relation to tree size in forests across the world. *New Phytologist* **234**, 1664–1677 (2022).
50. E. N. Broadbent. et al. The GatorEye Uninhabited Flying Laboratory: sensor fusion for 4D ecological analysis through custom hardware and algorithm integration. available at www.gatoreye.org/ (2023).
51. De Almeida, D. R. A. et al. Monitoring restored tropical forest diversity and structure through UAV-borne hyperspectral and lidar fusion. *Remote Sensing of Environment* **264**, 112582 (2021).
52. ESRI. ArcMap [Version 10.7.1]. Redlands, CA: Environmental Systems Research Institute (2019).
53. R Core Team. *R: A language and environment for statistical computing* (Version 4.1.3). R Foundation for Statistical Computing. https://www.R-project.org/ (2023).
54. Roussel, J. R. et al. lidR: An R package for analysis of Airborne Laser Scanning (ALS) data. *Remote Sensing of Environment* **251**, 112061 (2020).
55. J. R. Roussel, D. Auty, Airborne LiDAR Data Manipulation and Visualization for Forestry Applications R package version 4.0.1. https://cran.r-project.org/package=lidR (2022).
56. Tucker, C. Red and photographic infrared linear combinations for vegetation monitoring. *Remote Sensing of Environment* **8**, 127–150 (1979).
57. Huete, A. et al. Overview of the radiometric and biophysical performance of the MODIS vegetation indices. *Remote Sensing of Environment* **83**, 195–213 (2002).
58. Baldeck, C. A. & Asner, G. P. Estimating vegetation beta diversity from airborne imaging spectroscopy and unsupervised clustering. *Remote Sensing* **5**, 2057–2071 (2013).
59. Bates, D., Maechler, M., Bolker, B. & Walker, S. Fitting Linear Mixed-Effects Models Using lme4. *Journal of Statistical Software* **67**, 1–48 (2015).
60. J. Fox, S. Weisberg, An {R} Companion to Applied Regression, Third Edition. Thousand Oaks CA: Sage. URL: https://socialsciences.mcmaster.ca/jfox/Books/Companion/ (2019).
61. L. Komsta, F. Novometsky, moments: Moments, Cumulants, Skewness, Kurtosis, and Related Tests. R Package version 0.14.1. https://CRAN.R-project.org/package=moments (2022).
62. J. Gross, U. Ligges, nortest: Tests for Normality. R Package version 1.0-4. https://CRAN.R-project.org/package=nortest (2015).
63. Bayliss. et al. Data From: Scale-dependent responses to environmental fluctuations in tropical tree species' crown temperatures [Dataset]. Dryad. https://doi.org/10.5061/dryad.kwh70rzfp (2025).

Acknowledgements

Funding for this project was provided by the National Science Foundation (NSF #2026264) granted to Stephanie Pau (PI). We also wish to acknowledge the Pacific Southwest Research Station, the Institute of Pacific Islands Forestry, and Rob Hegemann for constant field support, Dr. Rebecca Ostertag and the Hawai'i Permanent Plot Network (HIPPNET) and the Hawai'i Experimental Tropical Forest. We also thank Franklin Sullivan (UNH) for helpful suggestions to improve our canopy architecture metrics. Most importantly, and with aloha, we would like to acknowledge the 'āina on which this work was carried out: the Laupāhoehoe forest in the moku of North Hilo.

Author contributions

Conceptualization: S.L.J.B., E.N.B., S.P.; Data Curation: E.N.B., S.L.J.B.; Formal Analysis: S.L.J.B.; Funding acquisition: S.P.; Investigation: E.N.B., S.L.J.B.; Methodology: S.L.J.B., E.N.B., S.P., A.M.A.Z.; Project administration: S.P.; Resources: E.N.B., A.M.A.Z., S.P., SC; Software: S.L.J.B., E.N.B.; Supervision: S.P.; Validation: E.N.B., S.P., A.M.A.Z., SC; Visualization: S.L.J.B.; Writing—original draft: S.L.J.B.; Writing—review & editing: S.L.J.B., S.P., E.N.B., A.M.A.Z., SC.

Competing interests

The authors declare no competing interests.

Ethics statement

This study was conducted with respect to the local communities and ecosystems in Hawai'i. We incorporate local language, which carries deep cultural and ecological significance, alongside scientific nomenclature to honor local heritage, promote accessibility, and foster greater community engagement with the research.

Additional information

Supplementary information The online version contains supplementary material available at https://doi.org/10.1038/s43247-025-02030-9.

Correspondence and requests for materials should be addressed to Shannon L. J. Bayliss.

Peer review information *Communications Earth & Environment* thanks Christopher E Doughty and the other, anonymous, reviewer(s) for their contribution to the peer review of this work. Primary Handling Editors: Mengjie Wang. A peer review file is available

Reprints and permissions information is available at http://www.nature.com/reprints

Publisher's note Springer Nature remains neutral with regard to jurisdictional claims in published maps and institutional affiliations.

Open Access This article is licensed under a Creative Commons Attribution 4.0 International License, which permits use, sharing, adaptation, distribution and reproduction in any medium or format, as long as you give appropriate credit to the original author(s) and the source, provide a link to the Creative Commons licence, and indicate if changes were made. The images or other third party material in this article are included in the article's Creative Commons licence, unless indicated otherwise in a credit line to the material. If material is not included in the article's Creative Commons licence and your intended use is not permitted by statutory regulation or exceeds the permitted use, you will need to obtain permission directly from the copyright holder. To view a copy of this licence, visit http://creativecommons.org/licenses/by/4.0/.

© The Author(s) 2025